Original paper

Prognostic impact of tumour budding, stromal phenotype, and CD163-positive macrophages in intestinal-type gastric adenocarcinoma

Elif Aydin[1], Ömer Atmiş[1], Hanife Seda Mavili[1], Mustafa Şahbazlar[2], Semin Ayhan[1]

[1]Department of Pathology, Faculty of Medicine, Manisa Celal Bayar University, Manisa, Turkey
[2]Department of Medical Oncology, Faculty of Medicine, Manisa Celal Bayar University, Manisa, Turkey

The tumour microenvironment plays an important role in the progression of gastric adenocarcinoma, but the prognostic value of its histopathological and immunological components in intestinal-type tumours remains unclear.
This retrospective study included 100 patients who underwent gastrectomy for intestinal-type gastric adenocarcinoma.
Tumour budding, stromal phenotype, tumour-stroma ratio, and lymphocytic infiltration were assessed on haematoxylin-eosin-stained sections, and immunohistochemical analyses of CD68, CD163, L-caldesmon, and periostin were performed at the invasive front. Tumour budding was associated with invasion depth and tumour stage but showed no independent prognostic significance. A myxoid stromal phenotype was independently associated with improved overall survival and reduced recurrence risk. CD163-positive macrophage density exceeded CD68 density and was independently linked to better survival. L-caldesmon expression was rare and not associated with clinicopathological parameters. Periostin expression correlated with macrophage infiltration but not with survival outcomes.
These findings suggest that stromal phenotype and tumour-associated macrophages, particularly CD163-positive cells, have prognostic relevance in intestinal-type gastric adenocarcinoma.

Key words: tumour budding, stromal phenotype, tumour microenvironment, gastric adenocarcinoma, CD163.

Introduction

Gastric cancer ranks as the fifth most frequently diagnosed malignancy worldwide and the fifth leading cause of cancer-related mortality globally. More than 90% of cases are adenocarcinomas [1, 2]. Owing to their marked morphological and histopathological heterogeneity, gastric cancers are currently classified most commonly according to the Lauren and World Health Organisation (WHO) systems [1]. Although surgical resection remains the cornerstone of curative treatment, it is insufficient as a sole modality in a substantial proportion of patients, necessitating the use of neoadjuvant or adjuvant therapies [3]. Nevertheless, overall survival (OS) rates remain unsatisfactory, underscoring the need for further investigation into novel prognostic markers and therapeutic targets, particularly those involved in tumour invasion and progression.

Tumour stage, depth of invasion, and lymph node metastasis constitute the principal determinants of prognosis in gastric cancer [4]. In addition, younger age [5], proximal tumour location [6], large tumour size [7], the presence of perineural invasion (PNI) and lymphovascular invasion (LVI) [8], and

positive surgical margins [9] have been identified as adverse prognostic factors. However, the impact of these conventional parameters on survival has shown considerable variability across studies, highlighting the necessity for exploring novel histological and stromal markers to improve prognostic stratification, particularly at the level of tumour subgroups.

In this context, tumour budding (TB), defined as isolated single tumour cells or small clusters of up to five cells detached from the main tumour mass at the invasive front, is regarded as a morphological manifestation of epithelial-mesenchymal transition (EMT) [10–12]. Tumour budding has been extensively investigated as a prognostic parameter across various organ systems and has been associated with poor clinical outcomes in multiple cancer types [13–15]. In gastric adenocarcinoma, TB has similarly been linked to depth of invasion, lymph node metastasis, and aggressive tumour behaviour; however, its independent prognostic value and its relationship with the tumour microenvironment (TME) have yet to be fully elucidated [16–18].

Recent advances in cancer biology have increasingly emphasised not only tumour-intrinsic oncogenic processes but also the critical role of tumour-stroma interactions in shaping disease behaviour. The tumour microenvironment comprises a complex network of cellular and acellular components, including extracellular matrix (ECM) elements, fibroblasts, and immune cells, all of which can directly influence tumour cell proliferation, invasive capacity, and metastatic potential [19, 20]. Despite this growing recognition, prognostic markers that clearly delineate the contribution of the stromal microenvironment to tumour progression in gastric cancer remain inadequately defined.

Among the key components of the TME, tumour-associated macrophages (TAM) play a pivotal role in regulating tumour progression and immune responses. While CD68 is widely used as a pan-macrophage marker, CD163 more specifically reflects the immunosuppressive M2 macrophage phenotype [21–23]. Microenvironments dominated by M2-polarised macrophages have been associated with enhanced tumour progression and invasive potential. Nevertheless, conflicting data have been reported regarding the prognostic impact of CD68- and CD163-positive macrophage infiltration in gastric adenocarcinoma, and the relationship of these markers with invasion and stromal features remains a subject of ongoing debate [24, 25].

L-caldesmon (L-CaD), an important component of the ECM and an actin-binding protein, is involved in various cellular processes, including apoptosis, cell motility, and adhesion [26, 27]. The *CALD1* gene produces two distinct isoforms, and L-CaD has been shown to be expressed in a wide range of non-smooth muscle cells. Although *CALD1* expression has been proposed to correlate with poor prognosis in certain tumour types, its association with the TME and clinical outcome in gastric cancer has not yet been clearly established [27, 28].

Periostin, another ECM protein secreted primarily by cancer-associated fibroblasts (CAF), has been implicated in regulating key processes within the TME, such as cell proliferation, angiogenesis, invasion, and metastasis [29, 30]. Elevated periostin expression has been linked to more aggressive tumour behaviour and increased mortality in several malignancies; however, studies specifically addressing the relationship between periostin expression and clinicopathological as well as stromal parameters in gastric cancer remain limited [31, 32].

In light of these considerations, the present study aimed to investigate the associations of TB, stromal phenotype, and tumour-associated macrophage infiltration with clinicopathological parameters and prognosis in intestinal-type gastric adenocarcinoma. In addition, periostin and L-CaD expression were evaluated as exploratory components of TME remodeling. Through this approach, we sought to achieve a more comprehensive understanding of the tumour microenvironmental elements contributing to the invasive process in intestinal-type gastric adenocarcinoma.

Material and methods

Study design and case selection

This study was designed as a retrospective, single-centre cohort study. Patients diagnosed with intestinal-type gastric adenocarcinoma who underwent total or subtotal gastrectomy between 2010 and 2020 at the Department of Pathology, Faculty of Medicine, Manisa Celal Bayar University, were included. Cases of mucinous carcinoma, signet ring cell carcinoma or tumours containing a signet ring cell component, undifferentiated carcinomas, and rare histological variants were excluded, as were patients who had received neoadjuvant therapy or whose pathological material or follow-up data were inadequate.

To minimise selection bias, 100 consecutive cases with available haematoxylin-eosin-stained slides and corresponding formalin-fixed and paraffin-embedded (FFPE) tissue blocks were enrolled. Clinical and follow-up data were retrieved from the Hospital Information System and the records of the Department of Medical Oncology. Demographic characteristics, type of surgery, clinical stage (AJCC), treatment details, recurrence status, lymph node and distant metastasis, OS, and disease-free survival (DFS) data were recorded.

Histopathological evaluation

All available haematoxylin and eosin (HE)-stained slides containing representative invasive tumour,

the invasive front, and adjacent stromal areas were re-evaluated. Histological tumour type and grade were assessed according to the 2019 WHO classification. Tumour invasion depth, lymph node status, and pathological stage were determined based on the 8th edition of the AJCC tumour-node-metastasis (TNM) staging system.

All histopathological assessments were performed independently by two pathologists who were blinded to clinical outcomes.

Tumour budding was defined as isolated single tumour cells or small clusters of up to five cells detached from the main tumour mass at the invasive front (Figures 1A–C) and was evaluated according to the criteria of the International Tumour Budding Consensus Conference (2016). All slides were initially screened at 10× magnification, and the areas with the highest budding density were selected and counted at 20× magnification. The number of tumour buds was normalised to an area of 0.785 mm^2. Budding was graded as follows: 0–4 buds (TB1), 5–9 buds (TB2), and ≥10 buds (TB3).

The desmoplastic stromal response was assessed at the invasive front and classified into three categories: fine fibrillary stroma (DR1), keloid-like stroma (DR2), and myxoid stroma (DR3) (Figures 1D–F). The tumour-stroma ratio was calculated in the area with the highest stromal content at the invasive front using 10% increments. Peritumoral and intratumoral lymphocytic infiltration were assessed based exclusively on mononuclear cells and scored semi-quantitatively as absent, mild, moderate, or marked. Absent was defined as no or only rare mononuclear inflammatory cells; mild as sparse mononuclear infiltrates with focal distribution; moderate as readily identifiable but not dense mononuclear infiltrates; and marked as dense and diffuse mononuclear infiltrates surrounding and/or permeating the tumour.

Immunohistochemical analysis

Immunohistochemical analysis was performed on sections obtained from FFPE tissue blocks containing the most invasive tumour areas (Figures 2A–D). Antibodies against CD68 (clone PG-M1), CD163 (clone MRQ-26), L-CaD (clone F-10), and periostin (clone F-10) were used. All immunostaining procedures were carried out on an automated immunohistochemistry platform in accordance with the manufacturers' protocols. Appropriate positive control tissues were included for each antibody in each staining run according to routine laboratory practice. Lymph node tissue was used as a positive control for CD68 and CD163, whereas non-neoplastic colonic wall tissue was used for L-CaD and periostin.

For CD68 and CD163, membranous and cytoplasmic staining was considered positive. For CD68 and CD163, the proportion of positive stromal macrophages at the invasive front was recorded in 10% increments. L-caldesmon staining was scored as 0 (no staining), 1 (weak/focal), or 2 (moderate/strong). Periostin expression was evaluated separately in the tumour centre and at the invasive front and classified using a three-tiered system (0–1–2).

Statistical analysis

Statistical analyses were performed using SPSS software version 23.0 (IBM Corp., Armonk, NY, USA). The distribution of continuous variables was assessed using the Shapiro-Wilk test. Continuous variables were expressed as mean ± standard deviation or median (minimum–maximum), as appropriate, while categorical variables were presented as number and percentage.

Associations between categorical variables were analysed using Fisher's exact test with Monte Carlo correction. The Mann-Whitney *U* test was applied for comparisons between two groups, and the Kruskal-Wallis test was used for comparisons involving three or more groups. Correlations were evaluated using Spearman's rho coefficient.

Overall survival was defined as the interval from the date of diagnosis to death or last follow-up, whereas DFS was defined as the time from diagnosis to the occurrence of recurrence or metastasis. Because cause-specific mortality data were not uniformly available, OS was analysed irrespective of cause of death. Survival analyses were performed using the Cox proportional hazards regression model. Variables found to be significant in univariate analyses were included in the multivariate model. A p-value < 0.05 was considered statistically significant.

Results

Demographic and clinical characteristics

A total of 100 patients were included in the study, comprising 31 females (31%) and 69 males (69%), with a mean age of 62.7 ±11.9 years (range: 37–86 years). Total gastrectomy was performed in 52 patients (52%), while 48 patients (48%) underwent subtotal gastrectomy (Table I).

The median follow-up period was 45.2 months (range: 1–162 months). During follow-up, 36 patients (36%) survived, whereas 64 patients (64%) died. The mean follow-up duration among deceased patients was 23.3 months. Recurrence data were available for 71 patients, among whom disease recurrence was observed in 31 cases (43.7%), with a mean time to recurrence of 20.1 ±14.9 months. The mean DFS was 47.9 ±45.2 months, and the mean OS was 53.2 ±42.9 months (Table I).

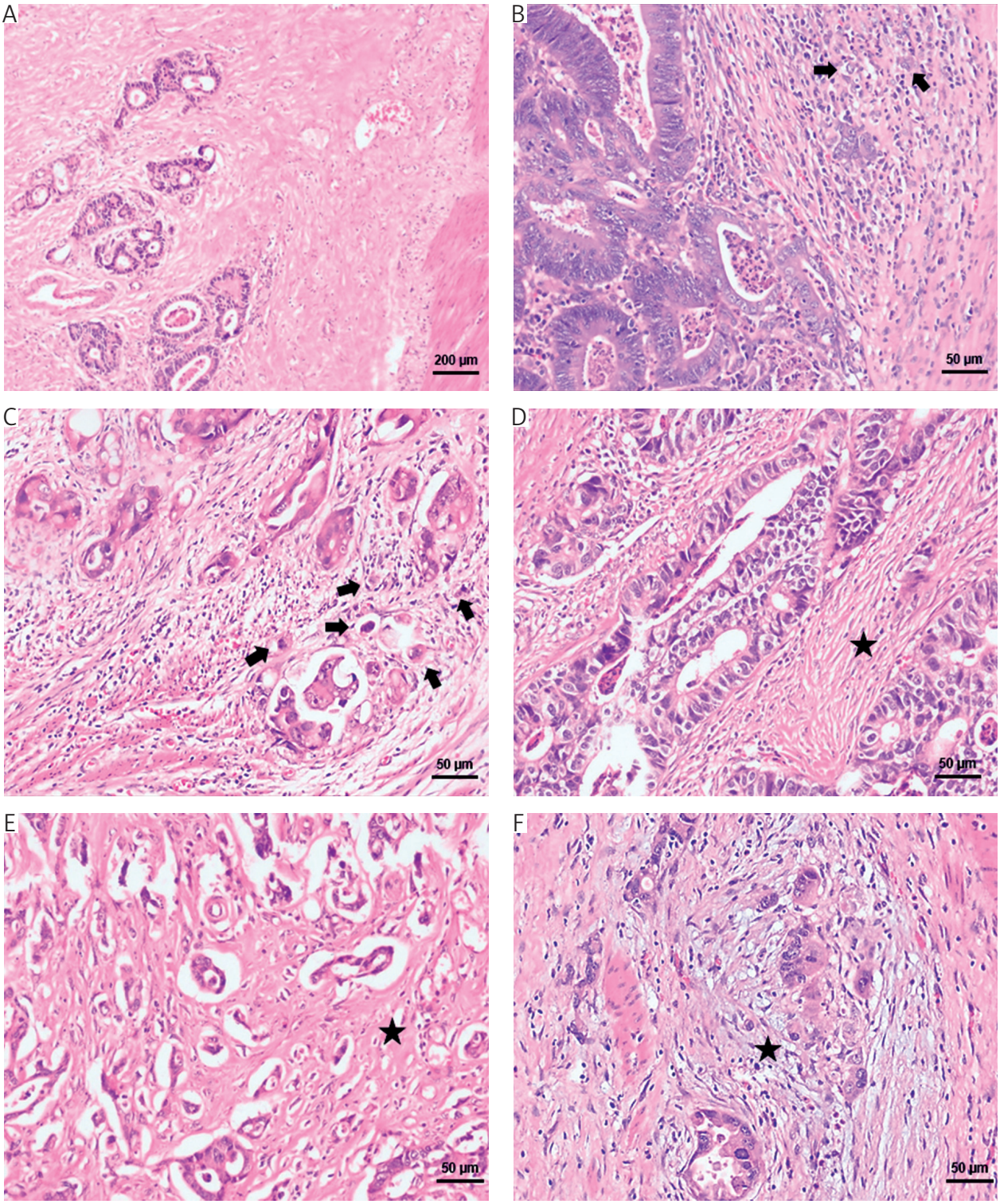

Figure 1. Representative histopathological features of tumour budding and stromal phenotype in intestinal-type gastric adenocarcinoma. Tumour budding (TB) was assessed according to the International Tumour Budding Consensus Conference (2016) criteria. **A**) Tumour area without identifiable tumour budding (HE, 40×). **B**) Tumour budding grade TB1 (0–4 buds) at the invasive front (arrows) (HE, 200×). **C**) Tumour budding grade TB2 (5–9 buds) at the invasive front (arrows) (HE, 200×). **D**) Fine fibrillary stromal phenotype characterised by delicate collagen fibres (asterisk) (HE, 200×). **E**) Keloid-like stromal phenotype with dense, eosinophilic collagen deposition (asterisk) (HE, 200×). **F**) Myxoid stromal phenotype showing loose, basophilic extracellular matrix (asterisk) (HE, 200×)

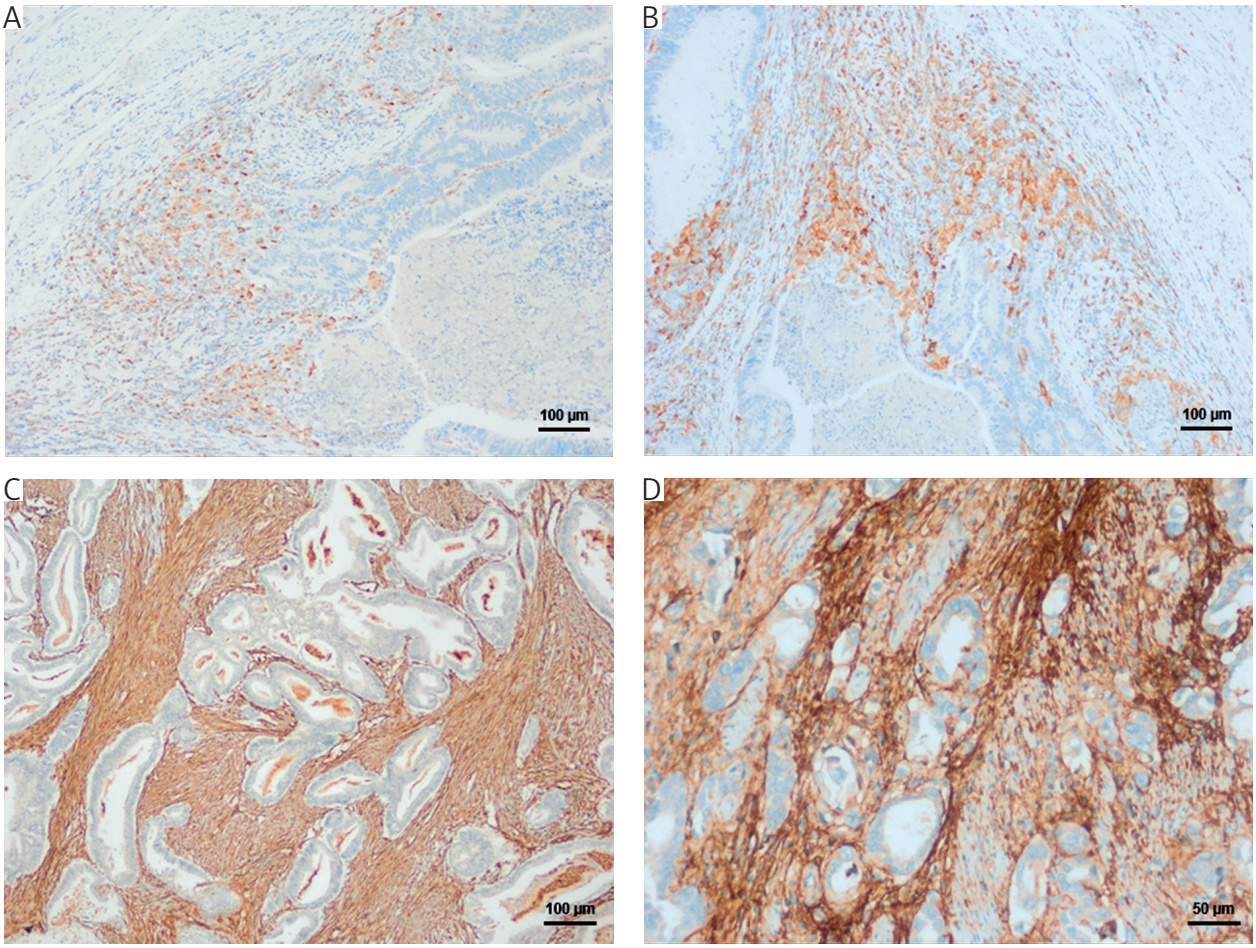

Figure 2. Immunohistochemical features of the tumour microenvironment in intestinal-type gastric adenocarcinoma. **A**) CD68 immunostaining demonstrating macrophage infiltration at the invasive front (100×). **B**) CD163 immunostaining showing a higher density of stromal macrophages compared to CD68 at the invasive front (100×). **C**) L-caldesmon immunostaining highlighting strong positivity in the muscularis propria as an internal control, with absence of staining in tumour cells (100×). **D**) Periostin immunostaining showing predominantly stromal expression without significant epithelial staining (200×)

Histopathological findings

Tumours were located proximally in 65 cases (65%) and distally in 35 cases (35%). The mean tumour size was 5.8 ±2.6 cm. With respect to histological subtype, the vast majority were tubular adeno-carcinomas (93%), followed by medullary (3%) and papillary carcinomas (4%). Seven tumours (7%) were well differentiated, while the remainder were moderately or poorly differentiated (Table I).

Four cases (4%) were classified as early-stage disease (pT1a–pT1b), whereas 96 cases (96%) were advanced-stage (pT2–pT4b). Lymph node metastasis (LNM) was detected in 77 patients (77%). The pathological nodal stages were distributed as follows: pN0 in 21%, pN1 in 15%, pN2 in 22%, pN3a in 27%, and pN3b in 15% of cases (Table I).

A significant association was observed between primary tumour stage and LVI ($p = 0.034$), as well as between primary tumour stage and PNI ($p < 0.001$). Pathological nodal stage was also significantly associated with primary tumour stage ($p = 0.039$). In addition, LVI was significantly correlated with pathological nodal stage ($p = 0.006$). No significant associations were identified between histological grade, peritumoral or intratumoral lymphocytic infiltration, and primary tumour stage ($p = 0.400$, $p = 0.507$, and $p = 0.772$, respectively).

Tumour microenvironment findings

Tumour budding

Tumour budding was observed in 92 cases, while 8 cases showed no budding. The mean tumour-stroma ratio at the invasive front was 46.4 ±28.6%, and the most frequent stromal pattern was fine fibrillary stroma (68%).

No significant association was found between TB and tumour location ($p = 0.792$). Tumours exhibiting TB were significantly larger than those without TB (4.8 cm vs. 3.2 cm, respectively; $p = 0.032$).

Table I. Clinicopathological characteristics of patients with intestinal-type gastric adenocarcinoma ($N = 100$)

Parameters	*n* (%) or mean ± SD	Parameters	*n* (%) or mean ± SD
Age [years]	62.7 ±11.9 (range 37–86)	Lymphovascular invasion	
Sex		Absent	24 (24)
Male	69 (69)	Present	76 (76)
Female	31 (31)	Perineural invasion	
Type of surgery		Absent	31 (31)
Total gastrectomy	52 (52)	Present	69 (69)
Subtotal gastrectomy	48 (48)	Tumour budding grade	
Tumour location		TB1	29 (29)
Proximal	65 (65)	TB2	45 (45)
Distal	35 (35)	TB3	26 (26)
Tumour size [cm]	5.8 ±2.6	Pathological T-stage	
Histological subtype (WHO)		pT1	4 (4)
Tubular adenocarcinoma	93 (93)	pT2	7 (7)
Papillary carcinoma	4 (4)	pT3	25 (25)
Medullary carcinoma	3 (3)	pT4a	59 (59)
Histological grade		pT4b	5 (5)
Well differentiated	7 (7)	Pathological N-stage	
Moderately differentiated	67 (67)	pN0	21 (21)
Poorly differentiated	26 (26)	pN1	15 (15)
Peritumoral lymphocytic infiltration		pN2	22 (22)
Mild	36 (36)	pN3a	27 (27)
Moderate	46 (46)	pN3b	15 (15)
Marked	18 (18)	Follow-up time [months]	45.2 (range 1–162)
Intratumoral lymphocytic infiltration		Overall survival [months]	53.2 ±42.9
Absent	27 (27)	Disease-free survival [months]	47.9 ±45.2
Mild	42 (42)	Recurrence	31 (43.7)
Moderate	29 (29)		
Marked	2 (2)		

SD – standard deviation, TB – tumour budding, WHO – World Health Organisation
Values are expressed as number (%) or mean ± standard deviation, as appropriate.

A significant relationship was also observed between histological grade and TB ($p = 0.037$) (Table II).

The tumour budding grade increased markedly with greater depth of invasion ($p < 0.001$). No TB3 cases were observed in pT1 or pT2 tumours, whereas TB3 was present in 37.3% of pT4a tumours and 40% of pT4b tumours. A significant association was identified between pathological tumour stage and TB ($p = 0.001$), while a borderline association was observed between nodal stage and TB ($p = 0.070$) (Table II). No significant associations were found between TB and tumour-stroma ratio, stromal phenotype, peritumoral lymphocytic infiltration, or intratumoral lymphocytic infiltration ($p > 0.05$).

Tumour stroma and macrophage infiltration

No significant associations were observed between stromal phenotype and LVI, PNI, depth of invasion, pathological tumour stage, or nodal stage ($p > 0.05$). In contrast, stromal phenotype showed significant correlation with macrophage infiltration. The median percentage of CD68-positive macrophages was 30% in tumours with fine fibrillary stroma and 10% in those with myxoid stroma ($p = 0.010$). Similarly, the median percentage of CD163-positive macrophages was significantly higher in fine fibrillary stroma (40%) than in myxoid stroma (20%) ($p < 0.001$) (Table IIIA).

Moreover, as the tumour-stroma ratio increased, the percentage of CD163-positive macrophages

Table II. Association of tumour budding with clinicopathological parameters

Parameters	TB1, *n* (%)	TB2, *n* (%)	TB3, *n* (%)	*p*-value
Histological grade				0.037
Well differentiated	3 (42.9)	1 (14.2)	3 (42.9)	
Moderately differentiated	24 (35.8)	29 (43.3)	14 (20.9)	
Poorly differentiated	2 (7.7)	15 (57.7)	9 (34.6)	
Lymphovascular invasion				0.057
Absent	10 (41.7)	12 (50.0)	2 (8.3)	
Present	19 (25.0)	33 (43.4)	24 (31.6)	
Pathological tumour stage				0.001
pT1	4 (100)	0 (0)	0 (0)	
pT2	5 (71.4)	2 (28.6)	0 (0)	
pT3	10 (40.0)	13 (52.0)	2 (8.0)	
pT4a	10 (16.9)	27 (45.8)	22 (37.3)	
pT4b	0 (0)	3 (60.0)	2 (40.0)	
Tumour-stroma ratio (%) (median, minimum–maximum)	60 (5–95)	50 (5–90)	45 (5–90)	0.811
Stromal phenotype				0.355
Fine fibrillary	23 (33.8)	31 (45.6)	14 (20.6)	
Keloid-like	3 (23.0)	5 (38.5)	5 (38.5)	
Myxoid	3 (15.8)	9 (47.4)	7 (36.8)	
CD68 (%) (median, minimum–maximum)	10 (5–70)	10 (5–80)	15 (5–70)	0.740
CD163 (%) (median, minimum–maximum)	20 (5–80)	30 (5–90)	20 (5–80)	0.837

TB – tumour budding
Categorical variables were compared using Fisher's exact or Monte Carlo tests, and continuous variables using Kruskal-Wallis test. Tumour-stroma ratio and immunohistochemical markers are presented as median (minimum–maximum).

decreased significantly ($r = -0.228$; $p = 0.023$), whereas no significant correlation was found between tumour-stroma ratio and the percentage of CD68-positive macrophages (Table IIIB).

Tumour-associated macrophages

At the invasive front, the mean percentage of CD68-positive macrophages was 19.8 ±19.6%, while the mean percentage of CD163-positive macrophages was 32.2 ±25.2%, indicating a predominance of CD163-positive macrophages (Figures 2A, B).

No significant associations were found between CD68 expression and histological grade, LVI, PNI, nodal stage, or depth of invasion ($p > 0.05$). Nevertheless, the percentage of CD68-positive macrophages increased from 7.5% in pT1 tumours to 26% in pT4b tumours.

CD163 expression was significantly associated with histological grade ($p = 0.019$) and PNI ($p = 0.030$). Although the association between CD163 and tumour stage did not reach statistical significance, CD163 expression showed a progressive increase with advancing stage (pT1: 15%; pT4b: 37%).

Both CD68-positive and CD163-positive macrophage percentages were significantly associated with peritumoral lymphocytic infiltration ($p = 0.001$ and $p < 0.001$, respectively). CD68 was also significantly associated with intratumoral lymphocytic infiltration ($p = 0.036$), and CD163 was likewise significantly associated with intratumoral lymphocytic infiltration ($p < 0.001$). Specifically, the mean percentage of CD163-positive macrophages increased from 18.5% in cases with mild lymphocytic infiltration to 52.2% in cases with marked lymphocytic infiltration.

L-caldesmon and periostin expression

L-caldesmon expression was negative in 92 cases (Figure 2C), weak/focal in 6 cases, and moderate-to-strong in 2 cases. No significant associations were found between L-CaD expression and any histological or microenvironmental parameters ($p > 0.05$). Given the limited number of positive cases, the clinical significance of this marker should be interpreted with caution.

Periostin expression was negative in the tumour centre in 74 cases, whereas only one case was negative at the invasive front, indicating significantly higher expression at the invasive front compared with the tumour centre. No significant associations were found between periostin expression and tumour stage, LVI, PNI, depth of invasion, or TB ($p > 0.05$). However,

Table III. Association between stromal phenotype and tumour-associated macrophages at the invasive front

A. Comparison by stromal phenotype

Stromal phenotype	CD68 median (minimum–maximum)	CD163 median (minimum–maximum)
Fine fibrillary	30 (5–90)	40 (5–90)
Keloid-like	20 (5–70)	30 (5–80)
Myxoid	10 (5–60)	20 (5–70)
p-value	0.01	< 0.001

B. Correlation with tumour-stroma ratio (Spearman's rho)

Parameters	*R*	*P*-value
CD68	–0.115	0.255
CD163	–0.228	0.023

CD68 and CD163 values are presented as median (minimum–maximum). Comparisons were performed using Kruskal-Wallis test. Spearman's rho was used for tumour-stroma ratio correlation analysis.

periostin expression was significantly correlated with both the percentages of CD68-positive ($p = 0.007$) and CD163-positive macrophages ($p < 0.001$).

Survival and recurrence analyses

Age was identified as an independent prognostic factor for OS ($p < 0.001$). Deeper invasion (muscularis propria: $p = 0.002$; serosa: $p = 0.009$) and lymph node metastasis (N3a and N3b, $p < 0.001$) were associated with significantly worse survival. Myxoid stroma was associated with a more favourable prognosis ($p = 0.036$) and remained an independent factor reducing the risk of recurrence in multivariate analysis ($p = 0.005$). The CD163-positive macrophage percentage was independently associated with improved OS in multivariate analysis ($p = 0.029$) (Table IV). No significant associations were observed between OS and TB, CD68, L-CaD, or periostin expression ($p > 0.05$).

With regard to DFS, age ($p = 0.001$) and lymph node metastasis (N3a and N3b, $p < 0.001$) were identified as independent prognostic factors, whereas TB, stromal phenotype, CD68, CD163, L-CaD, and periostin showed no significant associations with DFS ($p > 0.05$) (Table IV).

In terms of recurrence, LVI emerged as an independent risk factor in multivariate analysis ($p = 0.041$). Lymph node metastasis was the strongest prognostic factor for recurrence (N3a and N3b, $p < 0.001$). Tumour budding, CD68, CD163, L-CaD, and periostin expression were not significantly associated with recurrence ($p > 0.05$) (Table IV).

Discussion

In the present study, we performed a multidimensional assessment of histopathological and immunological components of the TME in intestinal-type gastric adenocarcinoma, examining the clinical and prognostic relevance of TB, stromal features, tumour-

Table IV. Multivariate Cox regression analysis for overall survival, disease-free survival, and recurrence

Parameters	OS HR (95% CI)	*P*-value	DFS HR (95% CI)	*P*-value	Recurrence HR (95% CI)	*P*-value
Age	1.073 (1.04–1.106)	< 0.001	1.043 (1.018–1.07)	0.001	–	–
Lymphovascular invasion	–	–	–	–	2.582 (1.038–6.421)	0.041
Pathological N-stage						
N1	–	–	3.436 (1.117–10.571)	0.031	7.47 (1.503–37.12)	0.001
N2	3.026 (1.045–8.761)	0.041	4.077 (1.461–11.378)	0.007	6.801 (1.466–31.547)	0.001
N3a	7.639 (2.74–21.293)	< 0.001	7.998 (2.975–21.508)	< 0.001	11.831 (2.536–55.19)	< 0.001
N3b	7.205 (2.38–21.808)	< 0.001	7.347 (2.539–21.261)	< 0.001	9.878 (1.914–50.968)	< 0.001
Myxoid stroma	0.436 (0.201–0.947)	0.036	–	–	0.201 (0.068–0.592)	0.005
CD163-positive macrophage percentage	0.982 (0.965–0.998)	0.029	–	–	–	–

DFS – disease-free survival, HR – hazard ratios, OS – overall survival
Hazard ratios with 95% confidence intervals are shown. Only variables with statistical significance in univariate analysis were included in the multivariate model. Dashes (–) indicate variables not retained in the final multivariate model.

associated macrophages, and the expression of L-CaD and periostin. Collectively, our findings suggest that – beyond conventional pathological parameters – stromal phenotype and macrophage infiltration may capture biologically and clinically meaningful aspects of disease behaviour in this setting.

Tumour budding showed a significant association with depth of invasion and pathological tumour stage, supporting the concept that TB may serve as a morphological surrogate of an invasive phenotype and tumour progression. Prior studies have reported that high-grade TB is associated with worse survival in intestinal-type gastric adenocarcinoma [17, 33]. Tumour budding is widely regarded as a morphological correlate of EMT, and EMT-activated tumour cells have been shown to exhibit enhanced migratory and invasive capacities [34, 35]. In our cohort, the significant association between histological grade and TB, together with the marked increase in TB3 in advanced-stage tumours, is consistent with this biological framework (Table II). The significant association of TB with depth of invasion and primary tumour stage supports its role as a morphological indicator of the invasive phenotype; however, TB was not identified as an independent prognostic factor for survival or recurrence in our cohort and should therefore be interpreted in conjunction with other pathological and stromal features rather than as a stand-alone prognostic marker. Notably, the literature on the prognostic value of TB in gastric cancer remains heterogeneous: while several large series and meta-analyses support an association between high TB and poor outcomes, others report a more limited or context-dependent effect [33, 36]. Differences in cohort composition, scoring methodology, stage distribution, and adjuvant treatment strategies may partly account for these discrepancies.

One of the most notable findings of our study was the significant relationship between stromal phenotype and clinical outcome. Specifically, myxoid stroma was associated with improved survival and a lower risk of recurrence, and it remained an independent factor in multivariate models (Table IV). These results reinforce the view that the stroma is not merely a passive scaffold but rather an active microenvironmental compartment capable of modulating tumour biology [20, 37]. Previous studies have similarly suggested that both the tumour-stroma ratio and stromal phenotype may influence prognosis [38, 39]. In our cohort, the absence of a significant association between stromal phenotype and pathological stage, invasion depth, or TB argues that stromal characteristics may exert biological effects that are not simply a byproduct of tumour progression. This observation raises the possibility that stromal phenotype may reflect not only tumour aggressiveness but also host-related tissue responses and microenvironmental remodeling [20, 37].

Our evaluation of TAM further highlights the complexity of immune-stromal interactions within the TME. The predominance of CD163-positive macrophages relative to CD68-positive macrophages, together with the finding that a higher CD163-positive macrophage percentage independently correlated with better OS, suggests that macrophage biology in gastric cancer may not be adequately captured by a simplified M1–M2 dichotomy. While high CD163+ TAM infiltration has been reported to carry prognostic significance in certain studies [40], meta-analytic evidence indicates that CD68-positive TAM often have a neutral association with OS, whereas macrophage polarisation states may better reflect clinically relevant immune contexture [25]. The roles of TAM in tumour progression, angiogenesis, and immune suppression have been emphasised previously [24, 41]. Moreover, the associations between CD163+ macrophage infiltration and other immune parameters support the notion that cross-talk among immune cell subsets meaningfully shapes tumour behaviour [42, 43]. Taken together, these findings underscore that intestinal-type gastric adenocarcinoma evolves within a complex immune-stromal network rather than a tumour-cell – only landscape.

L-caldesmon expression was negative in the vast majority of cases and did not show significant associations with clinicopathological, microenvironmental, or prognostic variables. This pattern may indicate a limited biological role for L-CaD in intestinal-type gastric adenocarcinoma, at least as assessed by our approach. The literature suggests that caldesmon isoforms participate in cytoskeletal regulation, yet stromal myofibroblasts and CAF – key drivers of ECM remodeling and invasion – often exhibit low or absent expression of certain smooth muscle lineage markers, reflecting the complexity and heterogeneity of stromal differentiation states [44–46]. In this context, the low number of L-CaD-positive cases in our cohort warrants cautious interpretation and supports the need for validation in larger series, ideally incorporating stromal cell subtype-specific markers to more precisely characterise microenvironmental compartments. Importantly, negative findings may still be informative because they help refine the panel of candidate biomarkers and clarify which stromal pathways are less likely to be clinically actionable in a given tumour type.

Periostin expression was markedly higher at the invasive front compared with the tumour centre (Figure 2D), suggesting a role in invasion-associated microenvironmental remodeling. Periostin is an ECM protein primarily secreted by CAF and has been implicated in proliferation, angiogenesis, invasion, and metastasis in multiple malignancies [29, 30, 47]. In colorectal cancer, stromal periostin expression has been linked to infiltrative growth patterns, poor differentiation, and

advanced TNM stage, supporting its potential role as an adverse prognostic marker [47]. In contrast, Zhang *et al*. [48] reported that stromal periostin expression in intestinal-type gastric adenocarcinoma correlated with CD163-positive TAM and that higher periostin levels were associated with better survival. Such divergent observations suggest that the clinical impact of periostin may be context-dependent, varying with tumour type, stromal composition, and the broader immune milieu. Furudate *et al*. [49] further proposed that periostin can promote M2-like macrophage polarisation, thereby shaping an immunosuppressive, tumour-promoting microenvironment. In our study, the strong association between periostin expression and both the percentages of CD68-positive and CD163-positive macrophages supports the plausibility of periostin-driven immune-stromal interplay. Overall, our data align with the interpretation that periostin may function less as a direct prognostic marker and more as a readout of microenvironmental remodeling – particularly at the invasive front – within intestinal-type gastric adenocarcinoma.

From a clinical standpoint, age, lymph node metastasis, and depth of invasion emerged as the most robust independent prognostic factors for OS and/or DFS, consistent with the established prognostic hierarchy in gastric cancer. The dominant impact of nodal status on DFS and recurrence further indicates that conventional pathological parameters remain central to risk stratification. Nevertheless, the association of stromal phenotype with survival and recurrence in multivariate analyses suggests that microenvironmental biology can translate into clinically meaningful outcomes and may provide incremental prognostic information when integrated with standard staging variables (Table IV).

This study has several limitations. Its retrospective, single-centre design may introduce selection and information biases, and the low positivity rate for certain immunohistochemical markers – particularly L-CaD – limits the strength of conclusions regarding their prognostic value. Moreover, although periostin was broadly expressed at the invasive front, the distribution of expression categories may still constrain subgroup-level inferences. Despite these limitations, the study has notable strengths, including restriction to a relatively homogeneous histological subtype (intestinal-type), a multidimensional evaluation of the microenvironment, and the concurrent analysis of survival and recurrence endpoints.

Conclusions

This study highlights the biological and clinical relevance of histopathological and immunological components of the TME in intestinal-type gastric adenocarcinoma. The significant association of TB with depth of invasion and primary tumour stage supports its role as a morphological indicator of the invasive phenotype; however, TB was not identified as an independent prognostic factor for survival or recurrence in our cohort and should therefore be interpreted in conjunction with other pathological and stromal features rather than as a stand-alone prognostic marker.

Notably, stromal phenotype – particularly the presence of myxoid stroma – was associated with improved survival and a reduced risk of recurrence, underscoring that the tumour stroma represents an active biological determinant rather than a merely structural component. Furthermore, the association of tumour-associated macrophages, especially CD163-positive cells, with stromal characteristics and prognosis indicates that immune-stromal interactions within the microenvironment may translate into clinically meaningful outcomes.

In contrast, L-CaD and periostin expression were not identified as independent prognostic indicators for survival or recurrence and may instead reflect microenvironmental remodeling in intestinal-type gastric adenocarcinoma.

Overall, stromal phenotype and tumour-associated macrophage infiltration emerge as promising parameters that may contribute to a more refined understanding of prognosis in this tumour type. Validation in larger, prospective cohorts is warranted to confirm these findings and explore their potential clinical applicability.

Disclosures

1. Institutional review board statement: This study was approved by the Ethics Committee of Manisa Celal Bayar University (approval decision no: 20.478.486/2274, dated: 28.02.2024).
2. Assistance with the article: This work was supported by the Scientific Research Project Office of Manisa Celal Bayar University (project number: 2024-035).
3. Financial support and sponsorship: None.
4. Conflicts of interest: None.
5. Declaration of generative AI and AI-assisted technologies in the manuscript preparation process: During the preparation of this manuscript, the authors used ChatGPT (OpenAI) for language editing and stylistic refinement. After using this tool, the authors carefully reviewed and edited the content and take full responsibility for the integrity and accuracy of the work.

References

1. Nagtegaal ID, Odze RD, Klimstra D, Paradis V, Rugge M, Schirmacher P, et al. The 2019 WHO classification of tumours of the digestive system. Histopathology 2020; 76: 182-188.
2. Bray F, Laversanne M, Sung H, Ferlay J, Siegel RL, Soerjomataram I, et al. Global cancer statistics 2022: GLOBOCAN estimates of incidence and mortality worldwide for 36 cancers in 185 countries. CA Cancer J Clin 2024; 74: 229-263.

3. Sexton RE, Al Hallak MN, Diab M, Azmi AS. Gastric cancer: a comprehensive review of current and future treatment strategies. Cancer Metastasis Rev 2020; 39: 1179-1203.
4. Brierley JD, Giuliani M, O'Sullivan B, Rous B, Van Eycken L. TNM classification of malignant tumours. 9th ed. NJ: Wiley-Blackwell, Hoboken 2025.
5. Berlth F, Bollschweiler E, Drebber U, Hoelscher AH, Moenig S. Pathohistological classification systems in gastric cancer: diagnostic relevance and prognostic value. World J Gastroenterol 2014; 20: 5679.
6. Sternberg SS, Mills SE, Carter D. Sternberg's diagnostic surgical pathology. 4th ed. Lippincott Williams & Wilkins, Philadelphia 2004.
7. Nakamura K, Kamei T, Ohtomo N, Kinukawa N, Tanaka M. Gastric carcinoma confined to the muscularis propria: how can we detect, evaluate, and cure intermediate-stage carcinoma of the stomach? Am J Gastroenterol 1999; 94: 2251-2255.
8. Hyung WJ, Lee JH, Choi SH, Min JS, Noh SH. Prognostic impact of lymphatic and/or blood vessel invasion in patients with node-negative advanced gastric cancer. Ann Surg Oncol 2002; 9: 562-567.
9. Rosai J. Rosai and Ackerman's surgical pathology. 10th ed. Mosby, Edinburgh 2011.
10. Grigore AD, Jolly MK, Jia D, Farach-Carson MC, Levine H. Tumor budding: the name is EMT. Partial EMT. J Clin Med 2016; 5: 51.
11. Li H, Xu F, Li S, Zhong A, Meng X, Lai M. The tumor microenvironment: an irreplaceable element of tumor budding and epithelial-mesenchymal transition-mediated cancer metastasis. Cell Adh Migr 2016; 10: 1-13.
12. Lugli A, Zlobec I, Berger MD, Kirsch R, Nagtegaal ID. Tumour budding in solid cancers. Nature Rev Clin Oncol 2021; 18: 101-115.
13. Liang F, Cao W, Wang Y, Li L, Zhang G, Wang Z. The prognostic value of tumor budding in invasive breast cancer. Pathol Res Pract 2013; 209: 269-275.
14. Koyuncuoglu M, Okyay E, Saatli B, Olgan S, Akin M, Saygili U. Tumor budding and E-Cadherin expression in endometrial carcinoma: are they prognostic factors in endometrial cancer? Gynecol Oncol 2012; 125: 208-213.
15. O'Connor K, Li-Chang HH, Kalloger SE, Peixoto RD, Webber DL, Owen DA, et al. Tumor budding is an independent adverse prognostic factor in pancreatic ductal adenocarcinoma. Am J Surg Pathol 2015; 39: 472-478.
16. Olsen S, Jin L, Fields RC, Yan Y, Nalbantoglu I. Tumor budding in intestinal-type gastric adenocarcinoma is associated with nodal metastasis and recurrence. Hum Pathol 2017; 68: 26-33.
17. Kemi N, Eskuri M, Ikäläinen J, Karttunen TJ, Kauppila JH. Tumor budding and prognosis in gastric adenocarcinoma. Am J Surg Pathol 2019; 43: 229-234.
18. Gulluoglu M, Yegen G, Ozluk Y, Keskin M, Dogan S, Gundogdu G, et al. Tumor budding is independently predictive for lymph node involvement in early gastric cancer. Int J Surg Pathol 2015; 23: 349-358.
19. Anderson NM, Simon MC. The tumor microenvironment. Curr Biol 2020; 30: R921-R5.
20. Kalluri R. The biology and function of fibroblasts in cancer. Nature Rev Cancer 2016; 16: 582-598.
21. Mantovani A, Marchesi F, Malesci A, Laghi L, Allavena P. Tumour-associated macrophages as treatment targets in oncology. Nature Rev Clin Oncol 2017; 14: 399-416.
22. Kim KJ, Wen XY, Yang HK, Kim WH, Kang GH. Prognostic implication of M2 macrophages are determined by the proportional balance of tumor associated macrophages and tumor infiltrating lymphocytes in microsatellite-unstable gastric carcinoma. PloS One 2015; 10: e0144192.
23. Biswas SK, Mantovani A. Macrophage plasticity and interaction with lymphocyte subsets: cancer as a paradigm. Nature Immunol 2010; 11: 889-896.
24. Gambardella V, Castillo J, Tarazona N, Gimeno-Valiente F, Martínez-Ciarpaglini C, Cabeza-Segura M, et al. The role of tumor-associated macrophages in gastric cancer development and their potential as a therapeutic target. Cancer Treat Rev 2020; 86: 102015.
25. Yin S, Huang J, Li Z, Zhang J, Luo J, Lu C, et al. The prognostic and clinicopathological significance of tumor-associated macrophages in patients with gastric cancer: a meta-analysis. PloS One 2017; 12: e0170042.
26. Alnuaimi AR, Bottner J, Nair VA, Ali N, Alnakhli R, Dreyer E, et al. Immunohistochemical expression analysis of caldesmon isoforms in colorectal carcinoma reveals interesting correlations with tumor characteristics. Int J Mol Sci 2023; 24: 2275.
27. Lee M-S, Lee J, Kim JH, Kim WT, Kim WJ, Ahn H, et al. Overexpression of caldesmon is associated with tumor progression in patients with primary non-muscle-invasive bladder cancer. Oncotarget 2015; 6: 40370.
28. Liu Y, Xie S, Zhu K, Guan X, Guo L, Lu R. CALD1 is a prognostic biomarker and correlated with immune infiltrates in gastric cancers. Heliyon 2021; 7: e07257.
29. Zhao Z, Zhang Y, Guo E, Zhang Y, Wang Y. Periostin secreted from podoplanin-positive cancer-associated fibroblasts promotes metastasis of gastric cancer by regulating cancer stem cells via AKT and YAP signaling pathway. Mol Carcinogen 2023; 62: 685-699.
30. Fan C, Wang Q, Kanei S, Kawabata K, Nishikubo H, Aoyama R, et al. Periostin from tumor stromal cells might be associated with malignant progression of colorectal cancer via Smad2/3. Cancers 2025; 17: 551.
31. Liu Y, Huang Z, Cui D, Ouyang G. The multiaspect functions of periostin in tumor progression. Adv Exp Med Biol 2019; 1132: 125-136.
32. Sung PL, Jan YH, Lin SC, Huang CC, Lin H, Wen KC, et al. Periostin in tumor microenvironment is associated with poor prognosis and platinum resistance in epithelial ovarian carcinoma. Oncotarget 2015; 7: 4036.
33. Xue C, Du Y, Li Y, Xu H, Zhu Z. Tumor budding as a predictor for prognosis and therapeutic response in gastric cancer: a mini review. Front Oncol 2023; 12: 1003959.
34. Bilić Z, Zovak M, Glavčić G, Mužina D, Ibukić A, Košec A, et al. The relationship between tumor budding and tumor deposits in patients with stage III colorectal carcinoma. J Clin Med 2024; 13: 2583.
35. Zlobec I, Lugli A. Epithelial mesenchymal transition and tumor budding in aggressive colorectal cancer: tumor budding as oncotarget. Oncotarget 2010; 1: 651.
36. Guo YX, Zhang ZZ, Zhao G, Zhao EH. Prognostic and pathological impact of tumor budding in gastric cancer: a systematic review and meta-analysis. World J Gastrointestin Oncol 2019; 11: 898.
37. Hanahan D, Coussens LM. Accessories to the crime: functions of cells recruited to the tumor microenvironment. Cancer Cell 2012; 21: 309-322.
38. Kemi N, Eskuri M, Herva A, Leppänen J, Huhta H, Helminen O, et al. Tumour-stroma ratio and prognosis in gastric adenocarcinoma. Br J Cancer 2018; 119: 435-439.
39. Ueno H, Shinto E, Kajiwara Y, Fukazawa S, Shimazaki H, Yamamoto J, et al. Prognostic impact of histological categorisation of epithelial-mesenchymal transition in colorectal cancer. Br J Cancer 2014; 111: 2082-2090.
40. Huang X, Pan Y, Ma J, Kang Z, Xu X, Zhu Y, et al. Prognostic significance of the infiltration of CD163+ macrophages combined with CD66b+ neutrophils in gastric cancer. Cancer Med 2018; 7: 1731-1741.
41. Li J, Sun J, Zeng Z, Liu Z, Ma M, Zheng Z, et al. Tumour associated macrophages in gastric cancer: From function and mechanism to application. Clin Transl Med 2023; 13: e1386.
42. Park JY, Sung JY, Lee J, Park YK, Kim YW, Kim GY, et al. Polarized CD163+ tumor-associated macrophages are asso-

ciated with increased angiogenesis and CXCL12 expression in gastric cancer. Clin Res Hepatol Gastroenterol 2016; 40: 357-365.
43. Qian S, Zhang H, Dai H, Ma B, Tian F, Jiang P, et al. Is sCD163 a clinical significant prognostic value in cancers? A systematic review and meta-analysis. Front Oncol 2020; 10: 585297.
44. Zeine R, Salwen HR, Peddinti R, Tian Y, Guerrero L, Yang Q, et al. Presence of cancer-associated fibroblasts inversely correlates with Schwannian stroma in neuroblastoma tumors. Mod Pathol 2009; 22: 950-958.
45. Otranto M, Sarrazy V, Bonté F, Hinz B, Gabbiani G, Desmouliere A. The role of the myofibroblast in tumor stroma remodeling. Cell Adh Migr 2012; 6: 203-219.
46. Council L, Hameed O. Differential expression of immunohistochemical markers in bladder smooth muscle and myofibroblasts, and the potential utility of desmin, smoothelin, and vimentin in staging of bladder carcinoma. Mod Pathol 2009; 22: 639-650.
47. Oh HJ, Bae JM, Wen XY, Cho NY, Kim JH, Kang GH. Overexpression of POSTN in tumor stroma is a poor prognostic indicator of colorectal cancer. J Pathol Transl Med 2017; 51: 306-313.
48. Zhang T, Han Z, Chandoo A, Huang X, Sun X, Ye L, et al. Low periostin expression predicts poor survival in intestinal type gastric cancer patients. Cancer Manag Res 2018; 11: 25-36.
49. Furudate S, Fujimura T, Kakizaki A, Kambayashi Y, Asano M, Watabe A, et al. The possible interaction between periostin expressed by cancer stroma and tumor-associated macrophages in developing mycosis fungoides. Exp Dermatolo 2016; 25: 107-112.

Address for correspondence

Ömer Atmış
Department of Pathology, Faculty of Medicine, Manisa Celal Bayar University
Hafsa Sultan Hospital
Manisa, Turkey
e-mail: omeratmis@hotmail.com